Efficiency and Threshold Characteristics of Spectrally Beam Combined High-Power Diode Lasers

Fangyuan Sun, Shili Shu, Guanyu Hou, Lijie Wang, Jun Zhang, Hangyu Peng, Sicong Tian, Cunzhu Tong, *Senior Member, IEEE*, and Lijun Wang

***Abstract*— The efficiency, threshold characteristics, and the stability of spectral beam combining (SBC) of diode laser array had been studied based on different output couplers (OC). It was found that the lower OC reflectivity, lower internal loss, and shorter cavity-length of emitter were helpful for the realization of high efficiency SBC in an external cavity. However, too low OC reflectivity would also result in an unstable combining with the characteristic of side lobes appeared in far-field and the degraded efficiency. The influence of OC reflectivity on threshold current, lasing spectra, and the beam quality of SBC was investigated and analyzed.**

***Index Terms*— Efficiency, laser diode array, threshold, spectral beam combining.**

I. Introduction

HIGH power broad-area diode lasers (BALs) are widely used for pumping solid state lasers and fiber lasers, material processing, security and defense, which are typically coupled into a fiber for easy use by beam shaping and combining techniques. Spectral beam combining (SBC) is an efficient method to improve the slow axis beam quality of BAL arrays. With the identical current operation, the beam quality comparable to the single emitter was demonstrated [1]–[3]. This technique is based on the diffraction optical elements fulfilling the combination of multiple diode lasers. By using this method, high power and beam quality diode lasers were demonstrated [4]–[7], such as continuous wavelength (CW) 30 W laser array with $M^2 = 2$ [5], 4 kW diode laser with beam quality of 3.5 mm $\times$ mrad [8], 3-5 μm mid-infrared quantum cascade lasers with M^2 of 1.5 [8], etc.. SBC had also been used for the power scaling of fiber lasers with power level of 8 kW to 10 kW [9], [10]. Modifying SBC yielded an excellent beam quality along the slow axis, as reported by several research groups. A spectrally beam combined tapered mini-bar with 12 emitters yielded an output power of 9.3 W and a M^2 value of 5.3 along the slow axis [11]. $M^2_{slow} \approx 2.4$ with an emission power of 0.56 W was realized via off-axis SBC of a mini-bar [12]. Another approach of off-axis SBC involves using two gratings to form a V-shaped resonator and has yielded an output power in excess of 10 W with $M^2_{slow} < 14$ [13]. A commercial off-the-shelf diode laser stacks were combined via SBC with a volume Bragg grating. This method has yielded an output power of 80 W with $M^2_{slow} \approx 26$ and $M^2_{fast} < 21$ [14].

SBC had been investigated in theory and experiment [15]–[18]. The mode competition, spectral linewidth, and the effect of feedback on the beam quality and spectrum of SBC had been analyzed by a numerical model [15]. The influence of aberration of transform lens [16], crosstalk [17] on the beam quality was studied in theory. A simple theoretical and experimental investigation on the relationship between the combining efficiency and reflectivity of output coupler (OC) of diode array was performed in SBC [18]. However, the detailed investigation on the energy conversion efficiency, beam quality, threshold and output characteristics of SBC is lacking, the approaches to improve the efficiency of SBC is especially desired.

In this paper, a theoretical model was proposed to analyze the stability and efficiency of SBC, the combining experiment was performed to investigate the influence of OC reflectivity on the power, threshold, efficiency, spectrum behavior and beam quality. The unstable combining was demonstrated in theory and experiment. The limiting factors of efficiency in SBC were discussed.

II. SBC Stability and Efficiency Limitation

A. SBC Stability

The experimental setup of SBC was illustrated schematically in Fig. 1. The external cavity is established by the rear facet of the laser bar and OC. The laser array was collimated respectively using the fast axis collimator (FAC)

Manuscript received March 1, 2018; revised November 28, 2018; accepted December 20, 2018. Date of publication January 1, 2019; date of current version January 21, 2019. This work was supported in part by the National Natural Science Foundation of China under Grant 61790584 and Grant 61774153, in part by the Project of Chinese Academy of Sciences under Grant ZDRW-XH-2016-4, and in part by the Jilin Provincial Foundation under Grant 20180519024JH. *(Corresponding author: Cunzhu Tong.)*

F. Sun and G. Hou are with the State Key Laboratory of Luminescence and Applications, Changchun Institute of Optics, Fine Mechanics and Physics, Chinese Academy of Sciences, Changchun 130033, China, and also with the Center of Materials Science and Optoelectronics Engineering, University of Chinese Academy of Sciences, Beijing 100049, China.

S. Shu, L. Wang, J. Zhang, H. Peng, S. Tian, C. Tong, and L. Wang are with the State Key Laboratory of Luminescence and Applications, Changchun Institute of Optics, Fine Mechanics and Physics, Chinese Academy of Sciences, Changchun 130033, China (e-mail: tongcz@ciomp.ac.cn).

Color versions of one or more of the figures in this paper are available online at http://ieeexplore.ieee.org.

Digital Object Identifier 10.1109/JQE.2018.2890287

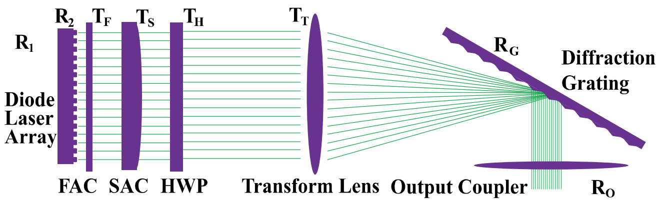

Fig. 1. Schematic diagram of the SBC of a diode laser array.

and slow axis collimator (SAC) due to the high divergence. Half wavelength plate (HWP) was essential to transfer the laser array's polarization from TM to TE. The combining of the laser array was achieved by a reflective diffraction grating (RDG). A Fourier transform lens (FTL) was used to image the beams into the RDG.

The SBC system just likes a three-mirror laser as show in Fig. 1. The front facet reflectivity of laser array R_2 cannot be neglected. The system with single element can be seen as a structure of hybrid resonator, then the effective complex reflection coefficient r_{eff} of the front facet of hybrid resonator can be expressed as [19], [20]

$$r_{eff} = \left(\frac{\sqrt{R_2}+\kappa\sqrt{R_0}e^{j\varphi_1}}{1+\kappa\sqrt{R_2}\sqrt{R_0}e^{j\varphi_1}}\right) \tag{1}$$

where $\varphi_1 = 4\pi L_b/n_b\lambda$. n_b is the refractive index of air, L_b is the length between the front facet of laser array and the OC, λ is the lasing wavelength. R_o is the reflectivity of OC. κ is the propagation loss factor from the optical lens, it's defined as

$$\kappa = T_F T_S T_H T_T R_G T_C \tag{2}$$

where T_F, T_S, T_H, T_T are respectively the transmissivities of FAC, SAC, HWP and FTL, R_G is the diffraction efficiency of RDG. Particularly, T_C is the couple efficiency of the light coupled back into the laser diode, which is less than 1 due to the aberrations and natural diffraction of the laser beams. At the threshold condition it satisfied

$$\sqrt{R}_1 r_{eff} e^{(g_{th}-a_i)L_a+j\varphi_0} = 1 \tag{3}$$

where $\varphi_0 = 4\pi L_a/n_a\lambda$. n_a is the refractive index of air, L_a is the length of array, g_{th} is the threshold modal gain, α_i is the absorption loss of active region. According to (3), it obtains

$$g_{th} = \alpha_i + \frac{1}{L_a}\ln\frac{1}{\sqrt{R_1 R_{eff}}}. \tag{4}$$

$$R_{eff} = \left(r_{eff} r^*_{eff}\right) = \left(\frac{\sqrt{R_2}+\kappa\sqrt{R_o}}{1+\kappa\sqrt{R_2}\sqrt{R_o}}\right)^2 \tag{5}$$

where R_{eff} is the reflectivity of front facet of the hybrid resonator, and increases with R_o. For the case of internal cavity of diode laser, i.e., $R_o = 0$, then $R_{eff} = R_2$, and the threshold becomes

$$g_{th0} = \alpha_i + \frac{1}{L_a}\ln\frac{1}{\sqrt{R_1 R_2}} \tag{6}$$

Here g_{th0} is the classical threshold gain of diode laser without external cavity. If it is quite small the feedback from the front facet of array compare with the external cavity feedback ($R_2 \approx 0$), from (4) and (5) we obtain

$$g_{thB} = \alpha_i + \frac{1}{L_a}\ln\frac{1}{\kappa\sqrt{R_1 R_o}} \tag{7}$$

where g_{thB} is the threshold modal gain of external cavity laser.

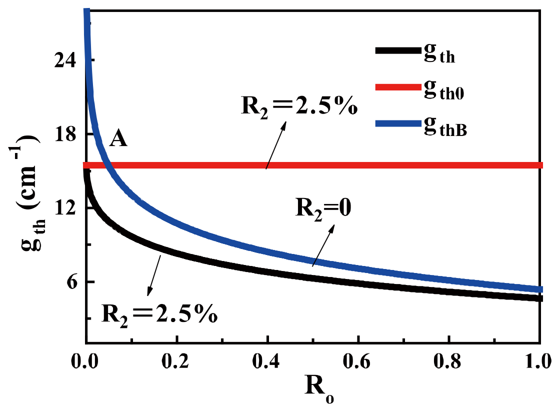

Fig. 2. Threshold modal gain as a function of the OC reflectivity.

The curve of threshold vs. the reflectivity of OC was calculated and shown in Fig. 2 with α_i of 3 cm^{-1}. g_{th0} represents the invariable threshold of laser array without any operation. The threshold modal gain of external cavity g_{thB} is inversely proportional to the reflectivity of OC. If the external cavity is locked stably, which must be satisfied that g_{thB} is much lower than g_{th0}. In other words, the value of the reflectivity of OC for stable combining should be larger than that of crossing point A shown in Fig.2, and it might be not stable for OC reflectivity close or lower than point A.

B. Efficiency Limitations

The output power and efficiency are crucial for beam combining. In general, the output power and energy conversion efficiency of SBC are lower than those of free running mode. To understand the affecting factors for the energy conversion efficiency of SBC, the following analysis was performed. The emission power of single emitters in a laser array can be written as [21]

$$P_i = \eta_{in}\left(\frac{hv}{q}\right)\left[\frac{-\ln\sqrt{R_1 R_{eff}}}{L_a g_{thi}}\right](I-I_{thi}) \tag{8}$$

where hv represents the energy band gap, q is the electronic charge. η_{in} is the internal quantum efficiency and determined mainly by the chip parameters, such as the stripe width, thickness of quantum wells, and barrier height. I is the injected current, I_{thi} is the threshold current. Assuming that all the emitters in the laser array are same, the energy conversion efficiency can be described as

$$\eta = \eta_{in}\left(\frac{hv}{q}\right)\left[\frac{-\ln\sqrt{R_1 R_{eff}}}{L_a g_{thi}}\right]\frac{(I-I_{thi})}{IV} \tag{9}$$

Here V is the voltage of laser array. Voltage performance is same for free running and SBC. R_{eff} is equal to R_2 for free running, and the energy conversion efficiency of laser array for both free running and SBC tends to be a saturated

TABLE I
PHYSICAL PARAMETERS OF DIODE LASER ARRAY

Symbol	Description	Values
R_1	rear facet reflectivity	95%
R_2	front facet reflectivity	2.5%
L_a	cavity length	1500 μm
T_F	transmissivity of FAC	95%
T_S	transmissivity of SAC	99.8%
T_H	transmissivity of HWP	99.8%
T_T	transmissivity of FTL	99.8%
R_G	diffraction efficiency of grating	95%
T_C	couple efficiency	~82.3%
f	focal length of FTL	200 mm
Λ	period of grating	1/1800 mm
θ_0	incident angle	57°
D	the spatial extend	9.5 mm
d	Emitter pitch	500 μm
w	Emitter width	100μm

maximum at high injected current [4], [6], so the ratio between the maximum energy conversion efficiency of SBC (η_s) and free running (η_f) can be written approximately as

$$\frac{\eta_s}{\eta_f} = \frac{\ln(R_1 R_{eff})}{\ln(R_1 R_2)} \frac{g_{th0}}{g_{th}}. \tag{10}$$

It can be found that the efficiency of SBC cannot be higher than that of free running due to the intrinsic characteristic of external cavity. The reflectivity of OC R_o, cavity length L_a, internal loss α_i and diffraction efficiency of grating R_G will all affect the value of η_s/η_f. Figure 3 shows the influence of R_o on η_s/η_f with different α_i and L_a. The physical parameters used were listed in Table I. In Fig. 3(a), the L_a is 1500 μm and the values of α_i are selected as 1 cm^{-1}, 3 cm^{-1} and 5 cm^{-1}, respectively. In Fig. 3(b), the internal loss α_i is 3 cm^{-1} and cavity length L_a is variable. It can be seen that η_s decreases with the increase of R_o, and higher internal loss and longer cavity length result in larger decrease, especially for high R_o. Hence, if expect high energy conversion efficiency in SBC, the diode laser array with low internal loss is desired. Although the short emitter cavity length is beneficial to realize a high η_s/η_f, it might lead to the low emission power and η_f if cavity length is too short. Figure 4 shows the influence of diffraction efficiency of grating R_G on η_s/η_f with different OC reflectivity R_o. The R_G plays more significant influence for η_s/η_f at high R_o. If select a low reflection OC in SBC, 10% difference in the diffraction efficiency of grating does not show the serious decrease on the combining efficiency. In brief, low reflectivity OC, low loss laser array and short emitter cavity length are helpful for high efficiency SBC.

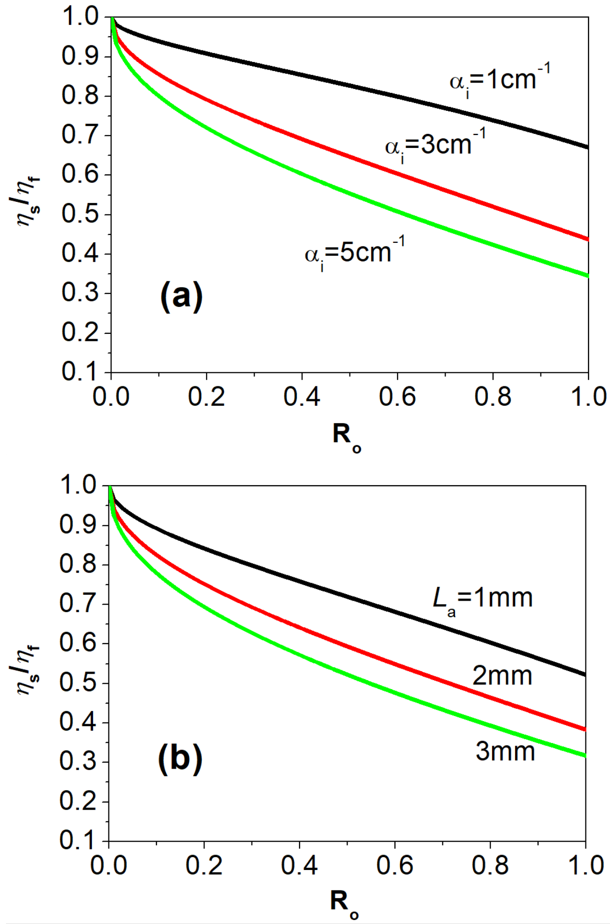

Fig. 3. The ratio between energy conservation efficiency of SBC and free running (η_s/η_f) as a function of R_o with different (a) internal loss α_i and (b) cavity lengthL_a.

III. EXPERIMENTAL RESULTS AND ANALYSIS

A. Power and Threshold Characteristics

Consider the strong dependence of SBC efficiency on the reflectivity of OC, the SBC of laser array with different OC was performed. The diode laser array consists of 18 emitters. The RDG is with 1-order diffraction efficiency of $\sim$ 95% for TE modes, the groove density of 1800 lines/mm and the blazing angle of 61.5°. The focal length of Fourier transform lens (FTL) is 200 mm. The other physical properties of the laser array used in the experiment were listed in Table I. Fig. 5 shows the power curves of laser array under free running and SBC with different OC reflectivity. The output power was measured under continuous wave (CW) operation at 17 °C. The OC with reflectivity of 6.8%, 14.4% and 33% were selected in SBC. These values of reflectivity were obtained by the realistic measurement. It can be seen the free running operation shows the highest output power, and the slope of curves increase with the decrease of OC reflectivity. However, the power curves of SBC with OC reflectivity of 6.8% and 14.4% are almost same. At a driving current of 50 A, the output power of free running is 38.5 W, the corresponding power of SBC are respectively 32.5 W, 31.7 W and 25.6 W for OC reflectivity of 6.8%, 14.4% and 33%. The slope efficiency of SBC is 0.74 W/A, 0.72 W/A and 0.58 W/A for OC reflectivity of 6.8%, 14.4% and 33%, respectively. The close power performance for OC reflectivity of 6.8% and 14.4% is conflicting with the predication of Eq.(10), the reason behind is the unstable combining for OC reflectivity of 6.8%, which will be discussed again in the part of far-field performance.

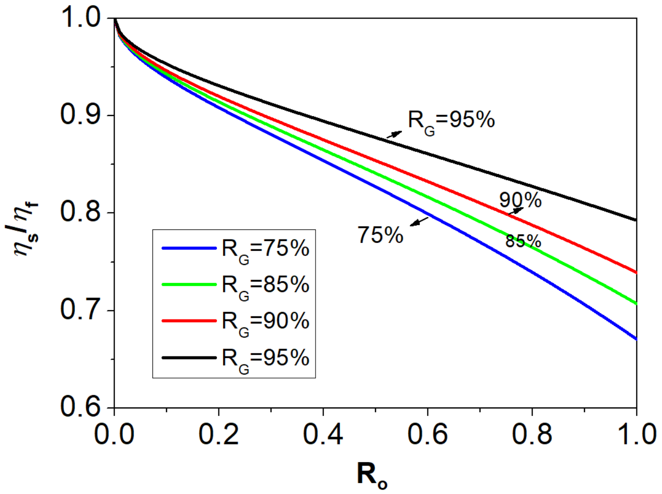

Fig. 4. The influence of diffraction efficiency of grating R_G on the ratio of η_s/η_f with different OC reflectivity R_o.

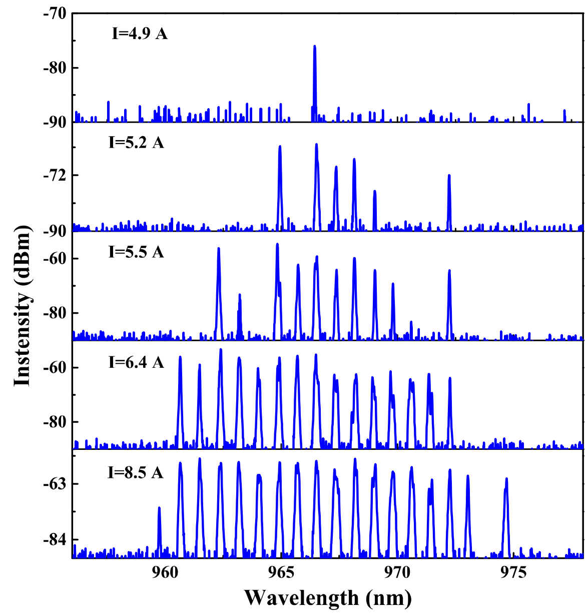

Fig. 6. Lasing spectra of SBC with OC reflectivity of 14.4% at different current.

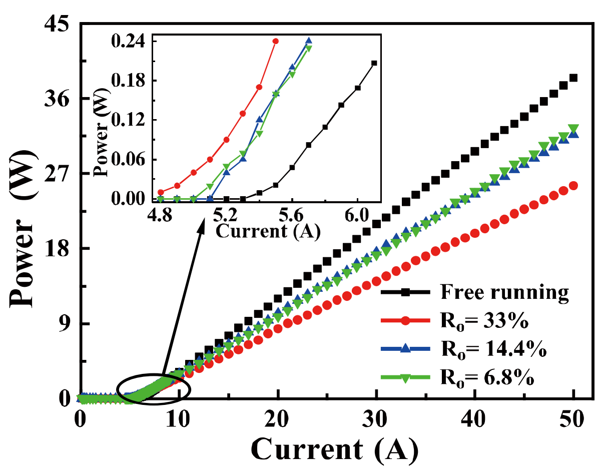

Fig. 5. Power performance of laser array under free running and SBC with different OC reflectivity. The inset shows the threshold characteristics.

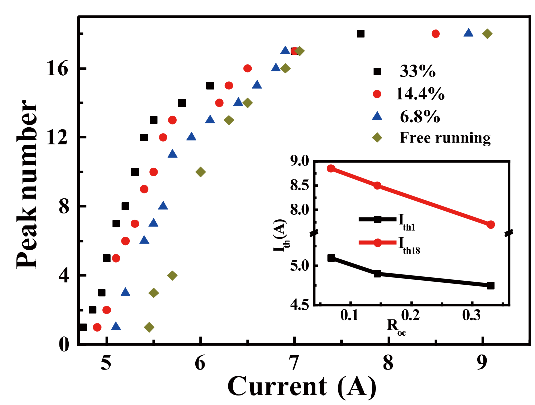

Fig. 7. Lasing of single emitter in free running and SBC with OC reflectivity of 33%, 14.4% and 6.8% as a function of injected current. Inset shows the dependence of threshold current of single emitter on the OC reflectivity R_o.

The inset of Fig. 5 shows the threshold characteristics. The SBC with OC reflectivity R_o of 33% represents the lowest threshold current due to the high feedback from OC. Free running shows the highest threshold current because the low feedback from the front facet with antireflection (AR) coating ($R_2 \sim 2.5$ %). The free running mode has the high threshold modal gain g_{th0}, but the mirror loss is also high. Hence it shows the high slope efficiency. Note that the threshold of lasing shown in the inset of Fig.5 is not steep, it is because the lasing threshold of single element in the laser array is not same totally. The lasing spectra of SBC with R_o of 14.4% were shown in Fig. 6 and disclose how the single emitter in laser array to lase in turn. At 4.9 A, the first emitting peak appears at the center position of spectrum. Then the other peaks appear from left and right sides in turn, the emitters at the edge of array are the last ones to lase, which means the light feedback in the external cavity of SBC is not uniform. In addition, there exists splits in some peaks, which indicates the slightly feedback crosstalk between the adjacent emitters [18].

The detailed threshold current for the single emitter in the laser array can be obtained from the measurement of lasing spectra and are shown in Fig. 7. The lasing of a single emitter is not linear dependence on the driving current, the last five or six emitters take more current. The high reflectivity of OC can reduce the threshold current and the difference between the first emitter (I_{th1}) and the last emitter (I_{th18}). The inset of Fig. 7 gives the influence of R_o on the threshold current $I_{th1}$and I_{th18}. The threshold current I_{th1} are respectively 4.6 A, 4.8 A and 5.2 A for the OC reflectivity of 33%, 14.4% and 6.8%. The corresponding I_{th18} are 7.5 A, 8.5 A and 8.8 A, respectively. It indicates that the lower OC reflectivity is corresponding to higher threshold current.

The wavelength interval Δd can be calculated by $\Delta d = (d\Lambda \cos \theta_0)/f$, and the obtained Δd is 0.826 nm, which is agreement with the measured value of 0.828 nm. The spectra width $\Delta\lambda$ can be expressed as $\Delta\lambda = (D\Lambda \cos \theta_0)/f$, which was determined by the focal length of FTL f, the dispersion of

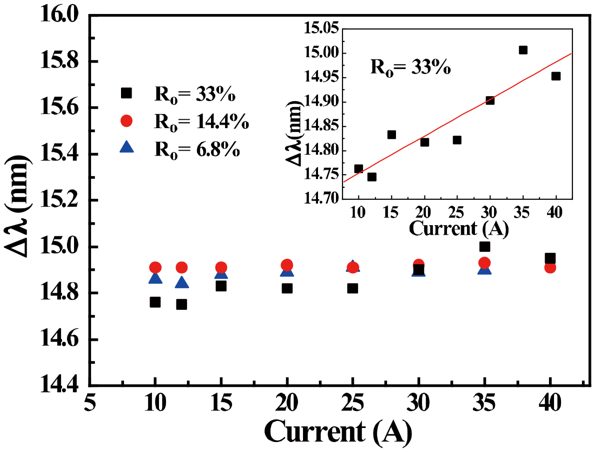

Fig. 8. The spectral width $\Delta\lambda$ as a function of current for the SBC of laser array with different OC reflectivity. The inset is the zoom-in curve for SBC with OC reflectivity of 33%.

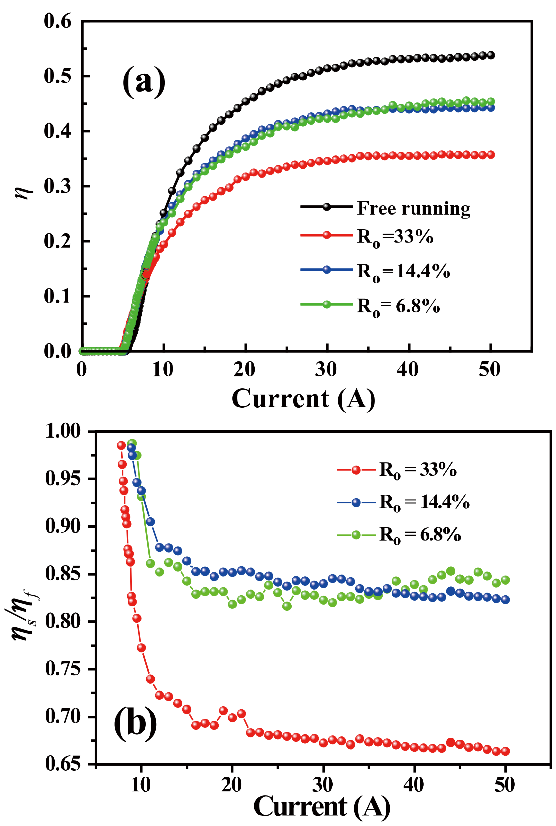

Fig. 9. (a) Energy conversion efficiency η and (b) combining efficiency η_s/η_f of laser array under the free running and SBC operation with R_o of 33%, 14.4% and 6.8% as a function of driving current.

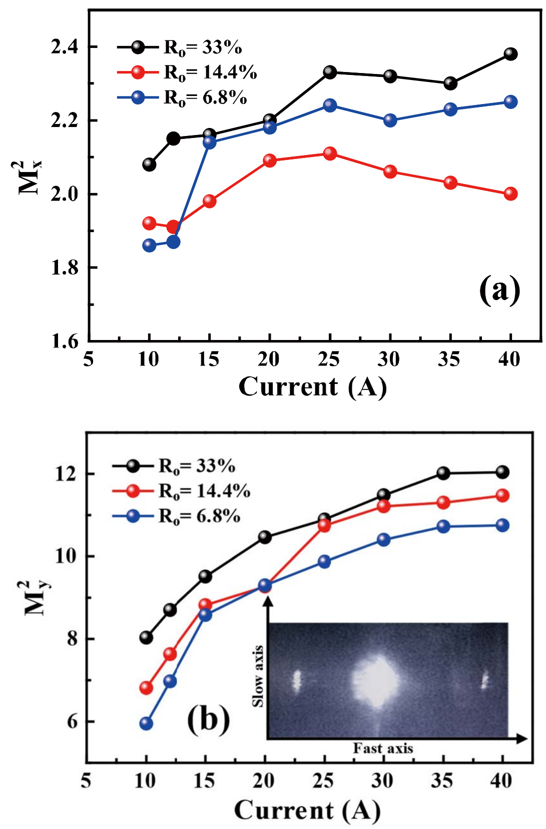

Fig. 10. M^2 factor in (a) the fast and (b) slow axes of SBC laser with OC reflectivity of 33%, 14.4% and 6.8%. The inset in (b) shows the far-field pattern of SBC with OC reflectivity of 6.8%.

grating, the spatial extend D and the incident angle relative to grating normal for center emitter. The calculated spectra width for our experimental configuration is 14.9 nm. The physical parameters used in Eqs. (11) and (12) are listed in Table I. The spectra width $\Delta\lambda$ curves measured by the spectrometer with the accuracy of 0.02 nm were shown in Fig. 8. For different OC reflectivity, the driving current shows a weak influence on $\Delta\lambda$, which was expended about 0.2 nm with the increased current of 30 A. The inset shows the expending spectra width $\Delta\lambda$ for $R_o = 33\%$, which was about 0.0075 nm/A and might be caused by the injection effect [22].

B. Efficiency

The measured energy conversion efficiency, η of SBC and free running of laser array were shown in Fig.9 (a). η increases with the driving current and reaches a stable maximum at high driving current. The laser array shows a high efficiency of 53.7% under free running. It is 35.7% for SBC with R_o of 33%. When R_o decreases to 14.4%, the maximum energy conversion efficiency of SBC (η_s) increases to 44.3%. Continue to reduce R_o to 6.8%, the maximum efficiency is almost unchanged ($\eta_s \sim 45.4\%$), which indicates the combining might be in the unstable region just as the theoretical predication in Fig.2. The ratio of η_s/η_f was shown in Fig.9 (b). It can be seen that η_s/η_f decreases with the increase of driving current, and reaches a stable value at high injection current. At 50 A, the combining efficiency η_s/η_f is about 85% for R_o ~6.8%. In contrast, they are respectively 82% and 66% for R_o of 14.4% and 33%. Note that SBC with R_o of 14.4% and 33% are in the stable region, and it can be deduced that the internal loss α_i is about 2.8 cm^{-1} from these experimental results according to Eq. (10). This value is reasonable for a high-power diode laser array. Above results reveal that low OC reflectivity is crucial for the realization of high efficiency SBC, however, the low OC reflectivity is not always beneficial to the high combining efficiency, especially when the OC reflectivity is less than 10%. It is because the combining becomes unstable for the low reflection OC. To demonstrate that, the far-field performance of SBC was measured.

C. Beam Quality and Stability

The beam quality of combined lasers can be described by M^2 factor, which was measured according to ISO11146 and plotted in Fig. 10 as a function of driving current with OC reflectivity of 33%, 14.4% and 6.8%. Fig. 10 (a) and (b) are respectively the M^2 factor in the fast (M_x^2) and slow axes (M_y^2). It can be seen M_x^2 was slightly varied with the increase of current, and SBC with OC reflectivity of 14.4% shows the best beam quality in spite of the small difference from those of OC reflectivity 33% and 6.8%. 33% reflectivity presents the worst beam quality in the fast axis. The relatively large difference happens in the slow axis as shown in Fig. 10 (b). M_y^2 increases with the current, which is a typical far-field blooming phenomenon [23]. For the OC reflectivity of 33%, M_y^2 increases from 8.0 to 12.0. At 40 A, M_y^2 are respectively 10.8, 11.5 and 12.0 corresponding to the OC reflectivity of 6.8%, 14.4% and 33%. Although SBC with OC reflectivity of 6.8% presents the best beam quality in slow axis, its far-field is not a clean single spot. There are two side lobes in the far-field as shown in the inset of Fig.10 (b), and the measured power of side lobe approaches to one watt. The measured power shown in Fig.5 does not include the power of side lobes. This phenomenon of side lobes does not happen in the SBC with high OC reflectivity. Hence, the beam combining with OC reflectivity of 6.8% is unstable and incomplete, which is in agreement with the theoretical predication shown in Fig. 2. To find the critical point of the far-field evolution in SBC with low OC reflectivity, the SBC with an OC reflectivity of 12.8% was performed. It also shows the side lobes in far-field, but the power of side lobes is in the order of several milliwatt. The accurate critical point is hard to obtain because the evolution happens gradually, but it should be between 6.8% and 12.8%.

IV. Conclusion

In summary, the threshold characteristics, efficiency and stability of SBC had been investigated based on different OC reflectivity. The theory predicates the existence of unstable combining when the threshold modal gain of external cavity in SBC is close to that of internal cavity. Experiments demonstrated that the combining became unstable when the OC reflectivity was less than 14.4%, and the far-field with side lobes appeared. It was shown that lower OC reflectivity, lower internal loss and shorter emitter cavity length were helpful for high efficiency SBC, and the efficiency increase with the decrease of OC reflectivity until the unstable combining region. Lower OC reflectivity is also beneficial to the beam quality based on the premise of stable combining. We believe these results will contribute to the development of high efficiency incoherent combining technology.

References

[1] A. Müller *et al.*, "16 W output power by high-efficient spectral beam combining of DBR-tapered diode lasers," *Opt. Express*, vol. 19, no. 2, pp. 1228–1235, Jan. 2011.

[2] X. Wu, Z. Ye, Z. K. Lu, Y. Takiguchi, Y. Wang, and H. Kan, "Beam combining of a high-power laser diode bar on a temperature gradient heat sink," *Chin. Opt. Lett.*, vol. 1, no. 2, pp. 93–95, Feb. 2003.

[3] Q. Zhou, C. H. Zhou, N. Yu, C. L. Wei, W. Jia, and Y. C. Lu, "Narrow-spectral-span spectral beam combining with a nonparallel double-grating structure," *Chin. Opt. Lett.*, vol. 15, no. 9, pp. 91403-1–91403-5, Sep. 2017.

[4] J. Zhang *et al.*, "CW 50W/M^2 = 10.9 diode laser source by spectral beam combining based on a transmission grating," *Opt. Express*, vol. 21, no. 3, pp. 3627–3632, Feb. 2013.

[5] R. K. Huang *et al.*, "High-brightness wavelength beam combined semiconductor laser diode arrays," *IEEE Photon. Technol. Lett.*, vol. 19, no. 4, pp. 209–211, Feb. 15, 2007.

[6] H. C. Meng *et al.*, "High-brightness spectral beam combining of diode laser array stack in an external cavity," *Opt. Express*, vol. 23, no. 17, pp. 21819–21824, Aug. 2015.

[7] D. Vijayakumar, O. B. Jensen, and B. Thestrup, "980 nm high brightness external cavity broad area diode laser bar," *Opt. Express*, vol. 17, no. 7, pp. 5684–5690, Mar. 2009.

[8] R. K. Huang *et al.*, "Teradiode's high brightness semiconductor lasers," *Pro. SPIE*, vol. 9730, P. 97300C, Apr. 2016.

[9] Y. Zheng *et al.*, "10.8 kW spectral beam combination of eight all-fiber superfluorescent sources and their dispersion compensation," *Opt. Express*, vol. 24, no. 11, pp. 12063–12071, May 2016.

[10] C. Wirth *et al.*, "High average power spectral beam combining of four fiber amplifiers to 8.2 kW," *Opt. Lett.*, vol. 36, no. 16, pp. 3118–3120, Aug. 2011.

[11] D. Vijayakumar, O. B. Jensen, R. Ostendorf, T. Westphalen, and B. Thestrup, "Spectral beam combining of a 980 nm tapered diode laser bar," *Opt. Express*, vol. 18, no. 2, pp. 893–898, Jan. 2010.

[12] O. B. Jensen, B. Thestrup, P. E. Andersen, and P. M. Petersen, "Near-diffraction-limited segmented broad area diode laser based on off-axis spectral beam combining," *Appl. Phys. B, Lasers Opt.*, vol. 83, no. 2, pp. 225–228, Feb. 2006.

[13] A. Jechow, V. Raab, and R. Menzel, "High cw power using an external cavity for spectral beam combining of diode laser-bar emission," *Appl. Opt.*, vol. 45, no. 15, pp. 3545–3547, May 2006.

[14] B. Chann, A. K. Goyal, T. Y. Fan, A. Sanchez-Rubio, B. L. Volodin, and V. S. Ban, "Efficient, high-brightness wavelength-beam-combined commercial off-the-shelf diode stacks achieved by use of a wavelength-chirped volume Bragg grating," *Opt. Lett.*, vol. 31, no. 9, pp. 1253–1255, May 2006.

[15] X. Tang, X. J. Wang, and W. W. Ke, "Numerical analysis of the beam quality and spectrum of wavelength-beam-combined laser diode arrays," *Proc. SPIE*, vol. 9255, p. 92551J, Feb. 2015.

[16] S. B. Zhan, Z. L. Wu, F. He, J. Zhang, J. C. You, and Y. W. Ma, "Influence of transform-lens focal length on spectral beam combining in an external cavity with a microlens array," *Opt. Commun.*, vol. 387, pp. 223–229, Mar. 2017.

[17] L. Yang, Z. Wu, Z. Q. Zhong, and B. Zhang, "Effect of crosstalk on combined beam characteristics in spectral beam combining systems," *Opt. Commun.*, vol. 384, pp. 30–35, Feb. 2017.

[18] Y. Q. Chen *et al.*, "Improving efficiency of spectral beam combining by optimizing reflectivity of output coupler for laser diode array," *Proc. SPIE*, vol. 10152, p. 101521F, Oct. 2016.

[19] A. Olsson and C. L. Tang, "Coherent optical interference effects in external-cavity semiconductor lasers," *IEEE J. Quantum Electron.*, vol. QE-17, no. 8, pp. 1320–1323, Aug. 1981.

[20] H. Sato and J. Ohya, "Theory of spectral linewidth of external cavity semiconductor lasers," *IEEE J. Quantum Electron.*, vol. QE-22, no. 7, pp. 1060–1063, Jul. 1986.

[21] M. W. Fleming and A. Mooradian, "Spectral characteristics of external-cavity controlled semiconductor lasers," *IEEE J. Quantum Electron.*, vol. QE-17, no. 1, pp. 44–59, Jun. 1981.

[22] C. Z. Tong, B. J. Bijlani, S. Alali, and A. S. Helmy, "Characteristics of edge-emitting Bragg reflection waveguide lasers," *IEEE J. Quantum Electron.*, vol. 46, no. 11, pp. 1605–1610, Nov. 2010.

[23] P. Crump, S. Böldicke, C. M. Schultz, H. Ekhteraei, H. Wenzel, and G. Erbert, "Experimental and theoretical analysis of the dominant lateral waveguiding mechanism in 975 nm high power broad area diode lasers," *Semicond. Sci. Technol.*, vol. 27, no. 4, p. 045001, Feb. 2012.

Fangyuan Sun received the B.S. degree in optical information science and technology from the Harbin Institute of Technology, Harbin, China, in 2012, and the MD–Ph.D. degree in condensed matter physics from the Changchun Institute of Optics, Fine Mechanics and Physics, Chinese Academy of Sciences, Changchun, China, in 2018.

His current research interests include high power, high brightness diode laser systems realized by spectral beam combining.

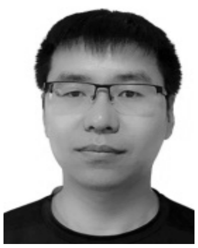

Shili Shu received the B.S. and Ph.D. degrees in materials from Jilin University, Changchun, China, in 2008 and 2013, respectively.

He joined the Changchun Institute of Optics, Fine Mechanics and Physics, Chinese Academy of Sciences, Changchun, in 2013. His current research interests include diode laser packaging and heat pipe.

Guanyu Hou received the B.E. degree from Nanjing Forestry University in 2012. He is currently pursuing the Ph.D. degree with the University of Chinese Academy of Sciences. His research interests are focused on the semiconductor disk lasers.

From 2013 to 2014, he was with the Changchun Institute of Optics, Fine Mechanics and Physics, Chinese Academy of Sciences, as a Technician.

Lijie Wang received the B.S. degree in optical communications from Jilin University, Changchun, China, in 2008, and the Ph.D. degree in condensed matter physics from the Changchun Institute of Optics, Fine Mechanics and Physics, Chinese Academy of Sciences, Changchun, in 2013. He is currently a Research Associate with the Changchun Institute of Optics, Fine Mechanics and Physics, Chinese Academy of Sciences.

His current research interests include high-brightness diode lasers, mid-infrared lasers, and photonic crystal lasers.

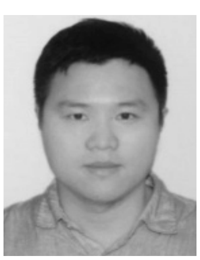

Jun Zhang received the B.S. degree from Jilin University in 2008 and the Ph.D. degree from the Changchun Institute of Optics, Fine Mechanics and Physics (CIOMP), Chinese Academy of Sciences, in 2013. He is currently with CIOMP, Chinese Academy of Sciences. His current research interests include high-power diode lasers coupling and its applications.

Hangyu Peng received the Diploma degree in physics from Beijing Jiaotong University, China, in 2005, and the Ph.D. degree from the Changchun Institute of Optics, Fine Mechanics and Physics, Chinese Academy of Sciences, in 2011. His current research interests include the packaging and beam combination of high-power diode lasers.

Sicong Tian received the B.S. and Ph.D. degrees in physics from Jilin University, Changchun, China, in 2007 and 2012, respectively.

He is currently a Research Associate with the State Key Laboratory of Luminescence and Application, Changchun Institute of Optics, Fine Mechanics and Physics, Chinese Academy of Sciences, Changchun. His current research interests include quantum optics, quantum dots, and photonic crystals.

Cunzhu Tong (M'09–SM'17) received the B.S. and M.S. degrees in physics from Chongqing University, Chongqing, China, and the Ph.D. degree in microelectronics and solid electronics from the Institute of Semiconductors, Chinese Academy of Sciences (CAS), Beijing, China.

He was a Research Fellow with Nanyang Technological University, Singapore, from 2005 to 2009. After that, he joined the Department of Electrical and Computer Engineering, University of Toronto, Toronto, ON, Canada, as a Post-Doctoral Researcher. He became a Professor in the Hundred Talents Program with CAS, Changchun, China. He was with the Changchun Institute of Optics, Fine Mechanics and Physics, CAS, in 2010. He has authored or co-authored over 90 refereed journal papers. He has presented numerous invited talks and tutorials. His current research interests include high-brightness diode lasers, photonic crystal lasers, and the beam combining of diode lasers.

Lijun Wang received the M.S. degree from the College of Electrical Science, Jilin University, Changchun, China, in 1973.

He was a Research Fellow with Jilin University until 1986. He joined the Changchun Institute of Optics, Fine Mechanics and Physics, Chinese Academy of Sciences (CAS), Changchun. From 1988 to 1989, he was with the Swiss Postal Telegraph and Telephone Agency, Bern, Switzerland. He was a Senior Visiting Scholar with Northwestern University, Chicago, IL, USA, from 1993 to 1995. Since 1995, he has been a Leading Professor with the Changchun Institute of Optics, Fine Mechanics and Physics, CAS. He has over 30 years of experience in the research of the semiconductor laser theory, technology, and applications. He holds over 30 Chinese patents. He has published over 400 papers and three academic books. He has hosted and participated in 15 national and ministerial important projects. His current research interests include high-power semiconductor lasers, vertical-cavity surface-emitting lasers, fiber-coupled diode lasers, and laser material processing. He received the National Science and Technology Progress Award, Second Prize once, the National Technological Invention Award, Second Prize once, and numerous other significant awards.